


# Floral cell discrepancy and CeABC subgroup member expression induction during scent release of *Cymbidium ensifolium*

Suying Zhan<sup>1#</sup>, Yukun Peng<sup>1#</sup>, Yinghui Cao<sup>1</sup>, Feihong Tang<sup>1</sup>, Yuqing Zhao<sup>1</sup>, Haiyan Wu<sup>1</sup>, Xiangwen Li<sup>1</sup>, Ruiliu Huang<sup>1</sup>, Kai Zhao<sup>2</sup>  and Yuzhen Zhou<sup>1\*</sup>

<sup>1</sup> The Cross-Strait Scientific and Technological Innovation Hub of Flower Industry, Key Laboratory of National Forestry and Grassland Administration for Orchid Conservation and Utilization at College of Landscape Architecture and Art, The Innovation and Application Engineering Technology Research Center of Ornamental Plant Germplasm Resources in Fujian Province, National Long Term Scientific Research Base for Fujian Orchid Conservation, Fujian Agriculture and Forestry University, Fuzhou 350002, China

<sup>2</sup> College of Life Sciences, Fujian Normal University, Fuzhou 350117, China

<sup>#</sup> Authors contributed equally: Suying Zhan, Yukun Peng

\* Corresponding author, E-mail: [zhouyuzhencn@fafu.edu.cn](mailto:zhouyuzhencn@fafu.edu.cn)

## Abstract

The floral scent of *Cymbidium ensifolium* is primarily composed of esters and terpenes, with peak emissions occurring at reproductive maturity and the highest levels observed in petals and sepals. Fatty acid-derived compounds such as methyl jasmonate (MeJA) dominate during full bloom, while less volatile sesquiterpenes increase in later stages, contributing to a lasting aroma. This study investigates the structural foundation in the formation of the *C. ensifolium* scent transportation process, including cell morphological changes and two key CeABCB transporter proteins. Microscopic observations indicated that the petal and sepal epidermis formed specialized cell structures. Specific transport proteins may mediate the membrane-based release of volatile compounds. Among 121 identified CeABC genes, CeABCB6 and CeABCG3 were highly expressed in petals and sepals, correlating strongly with the dynamics of volatile emissions. CeABCB6 and CeABCG3 were suggested to be involved in ATP-dependent MeJA transmembrane transport of substrates with different polarities based on their expression pattern and structural features. Both proteins are localized to the plasma membrane, supporting their roles in volatile transport. Additionally, CeABCG3 was significantly up-regulated under cold stress; its enhanced MeJA transport capability may be facilitated by changes in membrane fluidity or activation of abscisic acid (ABA) signaling pathways, contributing to environmental adaptation. Moreover, exogenous application of MeJA comparatively induced the expression of CeABCB6 and CeABCG3, supporting their potential involvement in MeJA-regulated floral scent regulation. This study highlights the critical roles of CeABCB6 and CeABCG3 in regulating floral scent and stress responses, laying a foundation for further exploration of volatile compound transport mechanisms.

**Citation:** Zhan S, Peng Y, Cao Y, Tang F, Zhao Y, et al. 2025. Floral cell discrepancy and CeABC subgroup member expression induction during scent release of *Cymbidium ensifolium*. *Ornamental Plant Research* 5: e035 <https://doi.org/10.48130/opr-0025-0031>

## Introduction

During floral scent emission in plants, endogenous volatile compounds accumulate substantially within cells, yet their intracellular concentrations show no direct correlation with release rates. The emission of volatile compounds requires their passage through biological membranes into the intercellular space or across the cuticle into the environment<sup>[1]</sup>. Passive diffusion alone may not be sufficient for the efficient release of volatile compounds, as differences in lipid solubility, membrane permeability, and cellular micro-environment can lead to intracellular retention. Therefore, plants must rely on efficient transmembrane transport mechanisms to regulate scent emission. The abundance of mitochondria in the epidermal cells in *Polianthes tuberosa* petals infers that volatile compound emission is an energy-dependent process<sup>[2]</sup>. Although plants can synthesize, store, and release volatiles through glandular structures such as trichomes and secretory cavities<sup>[3]</sup>, many floral organs lack these glands and rely on epidermal cells for scent synthesis and emission. Epidermal cell types in Orchidaceae are diverse. For instance, in *Dendrobium nobile*, petal epidermal cells can be classified into flat, semi-circular, elongated semi-circular, and papillate types<sup>[4]</sup>. These cell types are speculated to influence petal fragrance, color, humidity, and light reflection. In certain species, conical cells may work as trippers of volatile compounds<sup>[5]</sup>. Apart from cell morphology, active transport mediated by ABC

transporters also forms special transmembrane transports of volatile compounds and contributes to emission differences between the adaxial and abaxial petal surfaces<sup>[6,7]</sup>.

The ATP-binding cassette (ABC) transporter is one of the largest transporter families in living organisms. It is widely distributed in biological membranes such as the plasma membrane, vacuolar membrane, and peroxisomal membrane, facilitating the transmembrane transport of various substrates. They always play crucial roles in plant growth and development, secondary metabolite transport, and release of floral scent compounds<sup>[6,8,9]</sup>. For example, methyl jasmonate is synthesized from its precursor, oxylipin 12-oxo-phyto-dienoic acid (OPDA), which is transported into peroxisomes via ABC transporters located on the peroxisomal membrane in *Arabidopsis thaliana*, thereby promoting jasmonic acid biosynthesis<sup>[10]</sup>. Further research has revealed that AtABCG1 and AtABCG16 exhibit high substrate specificity for jasmonates (JA, MeJA, JA-Ile) and their precursors<sup>[11]</sup>. Among them, AtABCG16 is dually localized to both the plasma membrane and nuclear membrane, regulating intracellular jasmonate concentrations<sup>[12]</sup>. In addition, transmembrane release of volatile compounds mediated by ABC transporters is more efficient than simple diffusion and allows for the regulation of both the types and amounts of released volatiles<sup>[13]</sup>. In *Petunia hybrida*, ABC transporters have been confirmed to facilitate the release of floral volatiles<sup>[6]</sup>. Transient over-expression of the plasma membrane transporter gene *PhABCG1* increased volatile emission levels to

match those of the adaxial epidermis, indicating that the expression levels of transporters in different epidermal cell types are critical for the translocation of floral scent compounds<sup>[7]</sup>.

Members of the ABC transporter family contain Walker A, Walker B, and ABC signature motifs, as well as hydrophobic transmembrane domains (TMDs). A typical ABC transporter comprises two NBDs and two TMDs, forming the minimal functional unit for substrate transport. Half-size transporters, which contain only one NBD and one TMD, must homo-dimerize or hetero-dimerize to form a complete transport complex. Soluble ABC transporters that contain only NBDs can associate with membrane proteins containing only TMDs to form a half-molecule transport complex for functional transport. Additionally, these soluble ABC transporters may participate in processes such as DNA repair and gene expression regulation<sup>[14]</sup>. The NBD is responsible for binding and hydrolyzing ATP (adenosine triphosphate), while the TMD consists of multiple transmembrane  $\alpha$ -helices that form a substrate transport channel with sequence-specific substrate recognition. Upon substrate binding to the TMDs, the NBDs hydrolyze ATP to generate energy, driving the conformational changes required for transport. As ATP is bound and hydrolyzed by the NBDs, structural rearrangements occur in the TMDs, facilitating the translocation of substrate molecules across the membrane<sup>[15]</sup>.

With advancements in genomics, the ABC gene family has been fully identified in multiple plant species. Specifically, 129–225 ABC gene family members have been identified in the genomes of *A. thaliana*<sup>[16]</sup>, *Oryza sativa*<sup>[16]</sup>, *Capsicum annuum*<sup>[17]</sup>, *Solanum lycopersicum*<sup>[18]</sup>, *Brassica napus*<sup>[19]</sup>, and *Glycine max*<sup>[20]</sup>, respectively. Compared to other organisms, land plants possess more ABC transporters, which participate in various metabolic activities and contribute to their adaptation to complex environmental conditions<sup>[21]</sup>. The most commonly used classification method divides the plant ABC gene family into eight subfamilies (ABCA-ABCG and ABCI). However, ABCH-type genes were not identified in plants<sup>[22]</sup>.

The ABCG subfamily mainly consists of full-size and half-size transporters, characterized by an NBD-TMD reverse domain arrangement. With the exception of *AtABCG19*, ABCG transporters in *A. thaliana* are localized to the plasma membrane and are widely involved in plant growth, development, and stress responses<sup>[23]</sup>. *AtABCG16*, *AtABCG22*, *AtABCG25*, and *AtABCG31* participate in abscisic acid (ABA) transport and signaling<sup>[9, 24, 25]</sup>. *AtABCG14* is involved in cytokinin transport<sup>[26]</sup>, while *AtABCG16* mediates jasmonic acid (JA) efflux<sup>[12, 27]</sup>. Some ABCG transporters contribute to plant defense by regulating the salicylic acid (SA) and JA signaling pathways and secreting toxic compounds<sup>[28, 29]</sup>.

The fragrances of orchid flowers are diverse and mysterious<sup>[30]</sup>. In the previous identification and analysis of the ABC gene family in *Cymbidium ensifolium*, 121 ABC genes were identified. Two genes are closely related to functionally characterized ABCB and ABCG genes in *A. thaliana*, further supporting their potential roles in floral scent transport<sup>[31]</sup>. This study focuses on the functional mechanisms of ABC transporters in floral scent emission. As an important cultivated variety of Chinese orchids, *C. ensifolium* 'Xiaotaohong' emits a floral fragrance primarily composed of methyl jasmonate<sup>[32]</sup>. Given the critical role of ABC transporters in the transport of volatile compounds, this study systematically examines their functions in floral scent emission through floral micro-structure observation, ABC gene family identification, expression pattern analysis, and subcellular localization. The findings aim to provide theoretical foundations for elucidating the mechanisms underlying floral scent formation in orchids and offer genetic resources for fragrant breeding in Chinese orchids.

## Materials and methods

### Plasmids, strains, and plant materials

The plasmids pCambia1302-GFP and pGEX-6P-1 used in this study were preserved at the Key Laboratory of Orchid Conservation and Utilization, Fujian Agriculture and Forestry University. These plasmids were utilized for subcellular localization and *in vitro* protein expression, respectively. *Escherichia coli* DH5 $\alpha$  competent cells (B528413) and *Agrobacterium tumefaciens* GV3101 competent cells (B528430) were purchased from Sangon Biotech (Shanghai) Co., Ltd. The *C. ensifolium* 'Xiaotaohong' plants were obtained from Shancheng Town, Nanjing County, Zhangzhou City, Fujian Province, China (24° N, 117° E). Healthy, robust, and pest-free plants were selected for experimentation. Samples were collected at four distinct developmental stages: DL (bud stage), CK (initial blooming, day 0), SK (full bloom, day 4), and SB (senescence stage, day 10) (Figs 1a & 2a). At each stage, endogenous and emitted floral scent components were measured, with three biological replicates per group. To further investigate the specificity of floral scent emission and the regulatory functions of related genes, flowers at the full-bloom stage were dissected into four distinct floral organs: sepals, petals, labellum, and column. This dissection aimed to provide a deeper understanding of the floral scent emission characteristics of *C. ensifolium* 'Xiaotaohong'.

For subcellular localization experiments, leaves of *Nicotiana benthamiana* were used. Healthy young leaves from approximately 30-day-old plants were selected.

### Detection of floral scent components in *Cymbidium ensifolium* 'Xiaotaohong'

Volatile compounds were detected using the HS-SPME-GC-MS method. Fresh flower samples were placed at the bottom of a 15 mL head-space vial, and 1  $\mu$ L of ethyl decanoate solution (diluted in methanol) was added as an internal standard. The extraction fiber was inserted into the sample vial, positioned 1 cm above the sample, and exposed to a 35 °C water bath for 35 min for head-space adsorption. After adsorption, the fiber was inserted into the injection port of the gas chromatography-mass spectrometry (GC-MS) system (Shimadzu GC-MS-TQ8040) at 250 °C for desorption for 5 min, and the instrument was activated to collect data. Each sample was tested in triplicate.

The compounds released from the flowers were separated using chromatography, and a total ion current (TIC) chromatogram was generated. All TIC peaks were integrated, and substances were screened using a slope value of 1,000 and a half-peak width value of 2 as parameters. Each peak was annotated, and the corresponding mass spectra were retrieved. Qualitative analysis was performed by matching the retention indices and similarity scores with the NIST Mass Spectral Library and the FFNSC Flavors and Fragrances Library. Floral substances with a similarity index (SI) greater than 85 were retained. The identified floral scent compounds were cross-referenced with previously published plant volatiles in the Pherobase database (<https://pherobase.com>, accessed on 25 November 2023). The component content of volatile compounds was calculated by comparing the peak areas of the internal standard with the target compounds. The characteristic floral scents of the compounds were queried using the Perflavory database (<https://perflavory.com/>, accessed on 9 December 2023).

### Microscopic observation of floral structure

To comprehensively analyze the floral structures of *C. ensifolium* 'Xiaotaohong', a series of advanced microscopy techniques was employed to systematically examine its tissue structure and ultrastructural morphology. During the full-bloom stage, sepals and

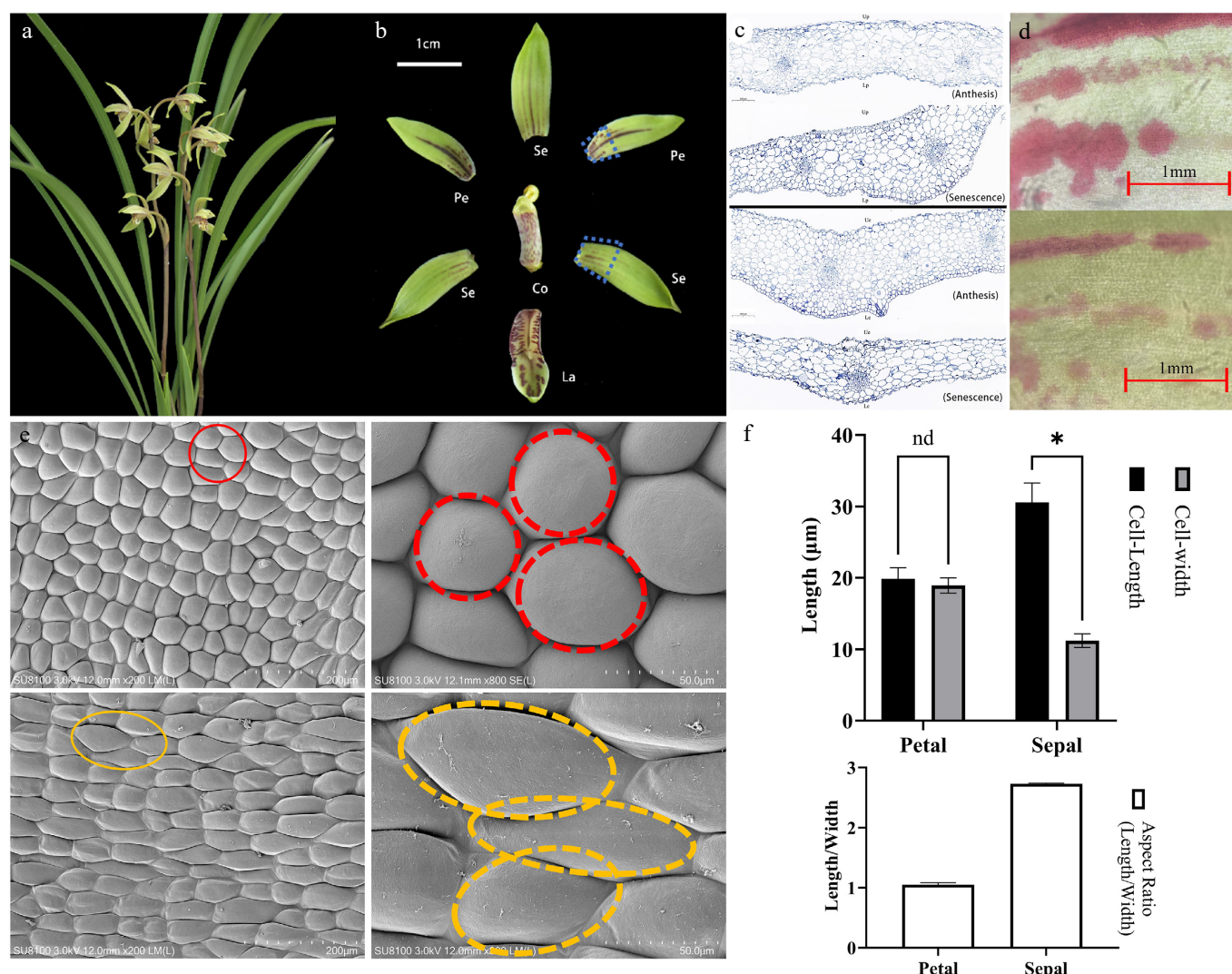


**Fig. 1** Microscopic observations of floral structures during the full bloom period of *C. ensifolium*. (a) Fully bloomed flowers. (b) Characteristics of different floral parts. Se, sepal; Pe, petal; La, labellum; Co, column. (c) Longitudinal structural diagram of petals and sepals. (d) Pigment distribution on the epidermis of sepals and petals at anthesis and senescence stages, visualized by light microscopy. (e) Scanning electron microscopy (SEM) images of petal and sepal epidermal cells. The red and yellow circles indicate typical polygonal cells and elongated cells, respectively. (f) Quantitative analysis of cell size in petal and sepal epidermis. Asterisks indicate statistically significant differences (\*,  $p < 0.0001$ ).

petals were selected as research materials and fixed in 2.5% glutaraldehyde solution overnight. The samples were then subjected to ethanol gradient dehydration, xylene clearing, and paraffin embedding, followed by sectioning. After staining, imaging was performed using a PANNORAMIC 250 Flash III DX panoramic scanner (3DHIS-TECH, Hungary) to observe histological characteristics.

For further analysis of the micro-structural features of the floral surface, samples were fixed sequentially with glutaraldehyde and osmium tetroxide, washed with phosphate buffer solution, and subjected to critical point drying. Subsequently, the samples were coated with a conductive metal layer to enhance conductivity. High-resolution images were obtained using a HITACHI-SU8100 scanning electron microscope (Hitachi High-Tech Corporation, Japan) to reveal the ultra-structural characteristics of the floral surface.

Additionally, to investigate the dynamic changes in cellular ultra-structure during floral development, floral tissues at the initial blooming, full-bloom, and senescence stages were subjected to transmission electron microscopy (TEM). Fresh samples were fixed in a low-temperature glutaraldehyde solution containing phosphate buffer, followed by osmium tetroxide fixation, ethanol gradient

dehydration, propylene oxide treatment, and resin embedding. After ultrathin sectioning and staining, imaging and analysis were conducted using an HT7700 transmission electron microscope (Hitachi High-Tech Corporation, Japan) to elucidate the ultra-structural changes occurring at the cellular level during floral development and senescence.

### Correlation analysis of CeABC gene expression and floral scent emission sites

To investigate the correlation between the expression of CeABC genes in different floral parts of *C. ensifolium* 'Xiaotaohong' and the emission of floral scent compounds, transcriptome expression analysis was conducted on 129 previously identified CeABC genes<sup>[31]</sup> (Supplementary Table S1). Transcriptome data were retrieved from the GSA BioProject, with accession numbers PRJCA009885/CRA007101 and PRJCA005426/CRA004351. Samples were collected from healthy plants (Fig. 1a). Flower samples were harvested on sunny and windless days between 10:00 and 12:00. Two types of sampling were performed: (1) whole flowers collected at nine developmental stages (e.g., DL, CK, SK, SB); (2) from fully open flowers on day 3 after anthesis, floral organs including petals, sepals, lips, and



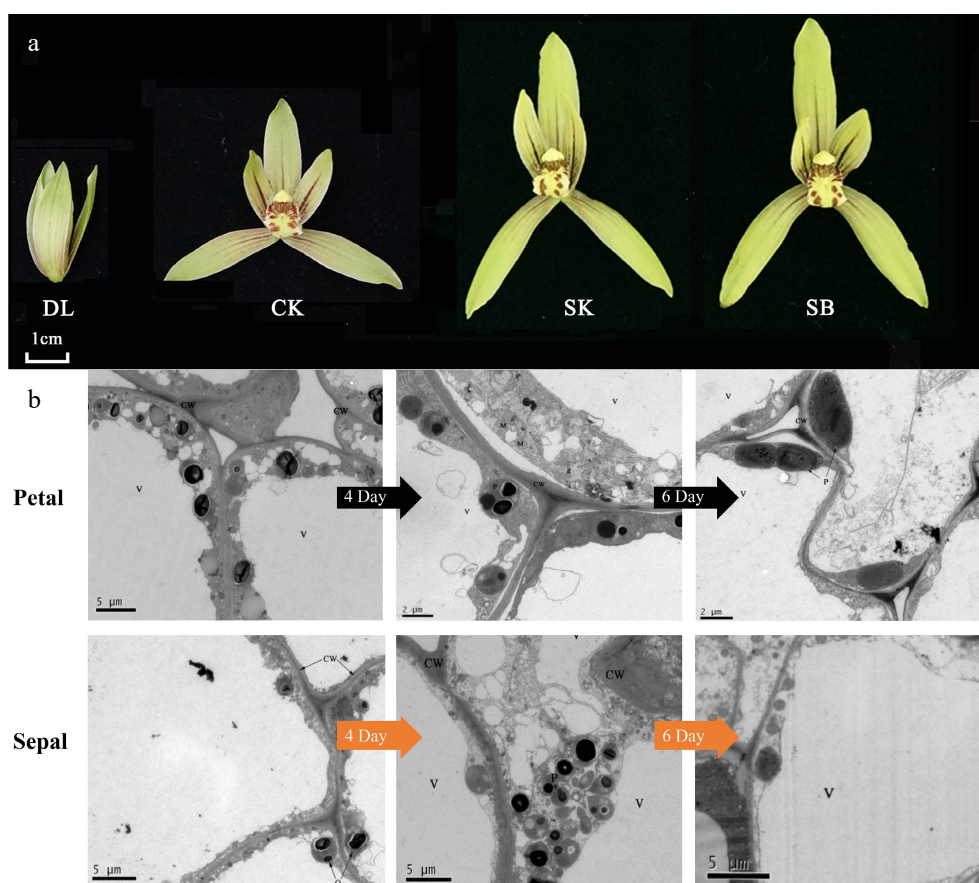


**Fig. 2** Developmental stages and ultrastructural characteristics of floral epidermal cells in *C. ensifolium*. (a) The nine blooming stages of *C. ensifolium*. DL (bud stage), CK (initial blooming, day 0), SK (full bloom, day 4), and SB (senescence stage, day 10). (b) Ultrastructural features of sepal and petal epidermal cells at different flowering stages. 4D and 6D refer to flowers that have been open for 4 d and 6 d, respectively. CW: cell wall; V: vacuole; P: plastid; M: mitochondrion.

gynostemium were separately collected, each with three biological replicates (Fig. 1b). Additionally, flowers at day 3 post-anthesis were sampled at seven time points across a 24 h period (0:00, 4:00, 8:00, 12:00, 16:00, 20:00, and 24:00), each with three replicates. Based on the MeJA content released from different floral parts, *CeABC* genes exhibiting specific expression patterns were selected for further validation using real-time quantitative PCR (RT-qPCR), followed by correlation analysis (Supplementary Table S2). Data visualization was performed using TBtools-II v2.119 and Origin2021.

### Phyicochemical properties and sequence alignment of *CeABC*B6 and *CeABC*G3 proteins

The physicochemical properties of the cloned *CeABC*B6 and *CeABC*G3 transporter proteins were analyzed using ProtParam. Structural domains of *CeABC*B6 and *CeABC*G3 were predicted using the SMART online tool (<http://smart.embl.de/>, accessed on 9 December 2023), while transmembrane domains were identified via the TMHMM online tool. Conserved nucleotide and amino acid sequences of all ABC proteins were analyzed using Maximum Likelihood (ML) and Bayesian Inference (BI) methods. The tertiary structures of *CeABC*B6 and *CeABC*G3 transporters were modeled using SWISS-MODEL. Homology searches for *CeABC*B6 and *CeABC*G3 transporters were performed using the NCBI online BLASTp tool. Multiple sequence alignments were conducted between *CeABC*B6 and *CeABC*G3 and their homologous ABC proteins from Orchidaceae species with high sequence similarity. Additionally, phylogenetic trees were constructed to infer protein functions, using *CeABC*B6 along with 28 *A. thaliana* ABCB transporters and *CeABC*G3 with 43 *A. thaliana* ABCG transporters.

### Temporal expression patterns of *CeABC* genes and their regulation under different stress conditions

During the full-bloom stage (the fourth day after anthesis), whole flowers of *C. ensifolium* 'Xiaotaohong' were sampled to investigate the temporal expression of *CeABC* genes. Sampling began at midnight (00:00) when flowers were fully open and continued every 4 h until 20:00 the following day. After each collection, samples were immediately flash-frozen in liquid nitrogen and temporarily stored at  $-80^{\circ}\text{C}$  for subsequent analysis. RStudio was used to analyze the expression levels of key genes (*CeABC*B6 and *CeABC*G3) associated with floral scent metabolism during anthesis, aiming to identify potential *CeABC* transcription factors involved in MeJA transmembrane transport in *C. ensifolium*.

To further explore the regulatory mechanisms of *CeABC* genes, fully opened flowers (the fourth day after anthesis) were treated with  $100\ \mu\text{mol/L}$  MeJA by foliar spraying. Whole flowers were collected at 0, 48, and 96 h after treatment, flash-frozen in liquid nitrogen, and stored at  $-80^{\circ}\text{C}$  to assess whether elevated MeJA concentrations induced feedback regulation of key *CeABC* gene expression.

Additionally, the study simulated environmental changes to examine their effects on *CeABC* gene expression. Fully bloomed *C. ensifolium* flowers were used as plant materials, with three biological replicates per treatment. Untreated flowers, maintained under identical growth conditions, served as the control group. The treatments included cold stress (flowers placed in a  $4^{\circ}\text{C}$  environment), ABA treatment (flowers sprayed with  $100\ \mu\text{mol/L}$  ABA solution)<sup>[33]</sup>, and drought stress (flowers immersed in a 20% PEG6000



solution)<sup>[34]</sup>. Samples were collected at 1, 3, and 7 d post-treatment, immediately frozen in liquid nitrogen, and stored at  $-80^{\circ}\text{C}$ . The temporal expression changes of these genes were quantified using RT-qPCR, with primer sequences provided in [Supplementary Table S2](#). Data visualization was performed using Origin 2021.

### Subcellular localizations of CeABCB3 and CeABCG6

The *CeABCB6* and *CeABCG3* genes were cloned from *C. ensifolium* 'Xiaotaohong' and inserted into the pCAMBIA1302-GFP vector. Homologous recombination was used to construct the recombinant vectors 1302-GFP-*CeABCB6* and 1302-GFP-*CeABCG3*, which were transformed into *Escherichia coli* DH5 $\alpha$  for positive clone screening. After plasmid extraction, the constructs were subsequently introduced into *Agrobacterium tumefaciens* strain GV3101. Additionally, a control vector expressing a plasma membrane-localized marker protein was constructed for comparison. Incubated at  $28^{\circ}\text{C}$  with shaking overnight, cells were harvested by centrifugation and resuspended in infiltration buffer (10 mM MES-KOH, pH 5.6; 10 mM  $\text{MgCl}_2$ ; 200  $\mu\text{M}$  acetosyringone) to an  $\text{OD}_{600}$  of 0.6–0.8, followed by incubation at  $28^{\circ}\text{C}$  in darkness for 3 h. Young *N. benthamiana* leaves were selected for infiltration, and the bacterial suspension was injected into the abaxial side of the leaves, avoiding major veins. After injection, leaves were incubated in darkness at  $25^{\circ}\text{C}$  for 8 h before being transferred to normal growth conditions (16 h light/8 h dark cycle). At 48–72 h post-infiltration, infiltrated leaf tissues were excised and mounted onto slides for GFP fluorescence observation using a Zeiss LSM880 confocal microscope. The fluorescence distribution of the control protein (pCAMBIA1302-GFP) was also examined to validate the reliability of the experimental system.

## Results

### Floral scent components in *C. ensifolium* 'Xiaotaohong'

A total of 79 volatile compounds were detected in the flowers of *C. ensifolium* 'Xiaotaohong' ([Supplementary Table S3](#)). The number of aromatic compounds released from the flowers at the early blooming, full blooming, and fading stages was 51, 59, and 67, respectively, with 37 aromatic compounds present in all three stages. The aromatic compounds were classified into the following categories: 26 fatty acid derivatives (a fatty aldehyde, three fatty alcohols, seven fatty acids, and 15 esters), 14 alkanes, 18 terpenes (seven irregular terpenes and 11 sesquiterpenes), 15 aromatic compounds, as well as other ethers, ketones, and alcohols. As the flowers opened, most of the compounds exhibited a pattern of first increasing and then decreasing. JA-Ile, jasmonic acid, and OPDA reached their highest levels in the early blooming flowers, while  $\alpha$ -linolenic acid and MeJA peaked in the full blooming flowers. In both the early and full blooming stages, the content of jasmonic acid and methyl jasmonate was significantly higher than that of other endogenous jasmonic acid-related compounds.

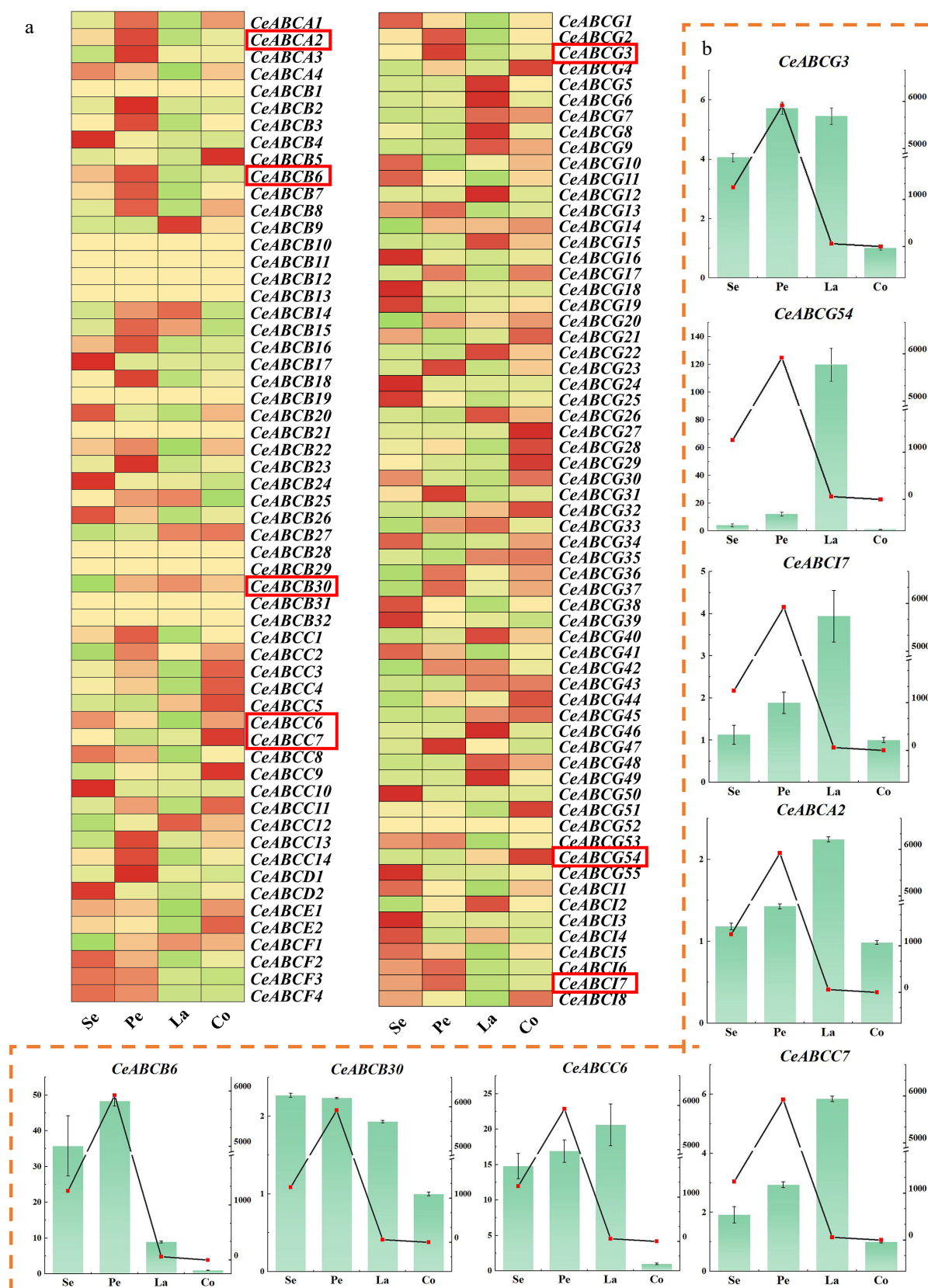
### Microscopic observation of floral cell structures

Previous studies have indicated that the sepals and petals of *C. ensifolium* 'Xiaotaohong' are the primary fragrance-releasing tissues during the full-bloom stage. In this study, multidimensional observations of the petals and sepals were conducted. Longitudinal structural images of sepals and petals during the blooming and fading stages revealed that the basic tissue cells of petals and sepals are nearly circular, with densely packed epidermal cells displaying irregular polygonal shapes. No specialized secretory structures were observed in the tissues ([Fig. 1c](#)). To complement the anatomical observations, light microscopy was employed to examine the surface of sepals and petals at the anthesis and senescence stages. The

results revealed the presence of distinct pigment distribution patterns, appearing as linear or spot-like accumulations on the epidermis, particularly in the petals ([Fig. 1d](#)). These pigmented regions correspond to areas of intense metabolic activity and may indicate sites of volatile precursor synthesis. The patterns were more prominent during anthesis and gradually faded as the flower aged, suggesting a potential link between pigmentation and volatile emission. Further SEM observations of epidermal morphology showed that the upper and lower epidermal cells of petals exhibit similar circular shapes with a smooth, slightly elevated surface ([Fig. 1e](#)). In contrast, the sepals' upper and lower epidermal cells were tightly packed, ovoid, and formed a honeycomb-like structure with slight outward convexity. Notably, no stomata or secretory structures were identified on either the upper or lower epidermis of sepals and petals, consistent with the longitudinal microscopic results. SEM observations revealed significant morphological differences between the petal and sepal epidermal cells of *C. ensifolium*. Petal cells were nearly round, with an aspect ratio ranging from 1.02 to 1.09, indicating a nearly spherical shape. In contrast, sepal cells exhibited an elongated, elliptical morphology with aspect ratios ranging from 2.72 to 2.76. These structural differences may reflect functional divergence between petals and sepals in development and light reflection, providing micro-structural evidence for floral morphological studies in orchids ([Fig. 1f](#)). To further investigate the sub-cellular structures of the primary fragrance-releasing tissues (sepals and petals), TEM was employed during the initial bloom, full bloom, and fading stages. The results showed that during the initial bloom, large central vacuoles occupied most of the epidermal cell volume, with organelles distributed near the cell membrane. Lipophilic osmiophilic particles began to accumulate in plastids ([Fig. 2b](#)). During the full-bloom stage, epidermal cells in sepals and petals exhibited developed organelles clustered near the cell membrane, and abundant lipid or lipophilic substances accumulated along the plastid boundaries, forming numerous osmiophilic particles. In the fading stage, epidermal cells of sepals displayed a high density of mitochondria and developed endoplasmic reticulum, but the central vacuole gradually reduced in size, and other organelles were loosely distributed. No osmiophilic particles were observed in plastids during this stage. At all stages, osmiophilic particles in the epidermal cells of sepals and petals were generated in locations consistent with the synthesis of MeJA, accumulating from organelle membranes to the cytoplasm and aggregating outward toward the membrane.

### The relationship between CeABC gene expression and the location of fragrance release

Transcriptome revealed that the expression of *CeABCs* exhibits significant tissue specificity within the floral organs of *C. ensifolium* ([Fig. 3a](#)). Among all 129 *CeABCs*, most *CeABCC* and *CeABCG* genes showed significantly higher expression levels in the gynostemium compared to other organs, while other gene categories were predominantly expressed in petals and sepals. This suggests that different branches of *CeABC* genes follow distinct expression patterns in various floral organs. Genes with strong tissue-specific expression were selected, including *CeABCG3*, *CeABCG54*, *CeABC17*, *CeABCA2*, *CeABCB3*, *CeABCB30*, *CeABCC6*, and *CeABCC7*. Using RT-qPCR, their expression levels were accurately quantified, and correlation analysis was performed with MeJA release in different floral parts ([Fig. 3b](#)). The results indicated that *CeABCB6*, *CeABCB30*, and *CeABCG3* were primarily expressed in petals and sepals, consistent with the fragrance release pattern. *CeABCG54* showed significantly higher expression in lips compared to all other genes, suggesting a unique function. These genes were thus selected for further regulatory analysis and sequence alignment.



## Structural characterization and subcellular localization of CeABCB6 and CeABCG3 proteins

Both CeABCB6 and CeABCG3 are members of the ABC transporter family and share high sequence identity with homologous proteins in other Orchidaceae species. CeABCB6 encodes 1,293 amino acids, while CeABCG3 encodes 1,435 amino acids, consistent with typical ABC transporter sizes (Supplementary Table S4). Multiple sequence alignment showed over 80% identity with other orchid ABC transporters (Supplementary Figs S1 & S2), and phylogenetic analysis

placed CeABCB6 near AtABC3/4/5/7/9/11/12/21, and CeABCG3 closer to AtABCG40 (Fig. 4a, b). Conserved domain analysis revealed that both proteins contain two nucleotide-binding domains (NBDs), each composed of a Walker A motif, a Walker B motif, and an ABC signature motif. Based on TMHMM predictions, CeABCB6 is expected to contain 11 transmembrane helices and adopt a canonical 'TMD–NBD' topology, while CeABCG3 harbors 13 transmembrane helices with an inverted 'NBD–TMD' arrangement. Predicted secondary structure composition was dominated by  $\alpha$ -helices and coils

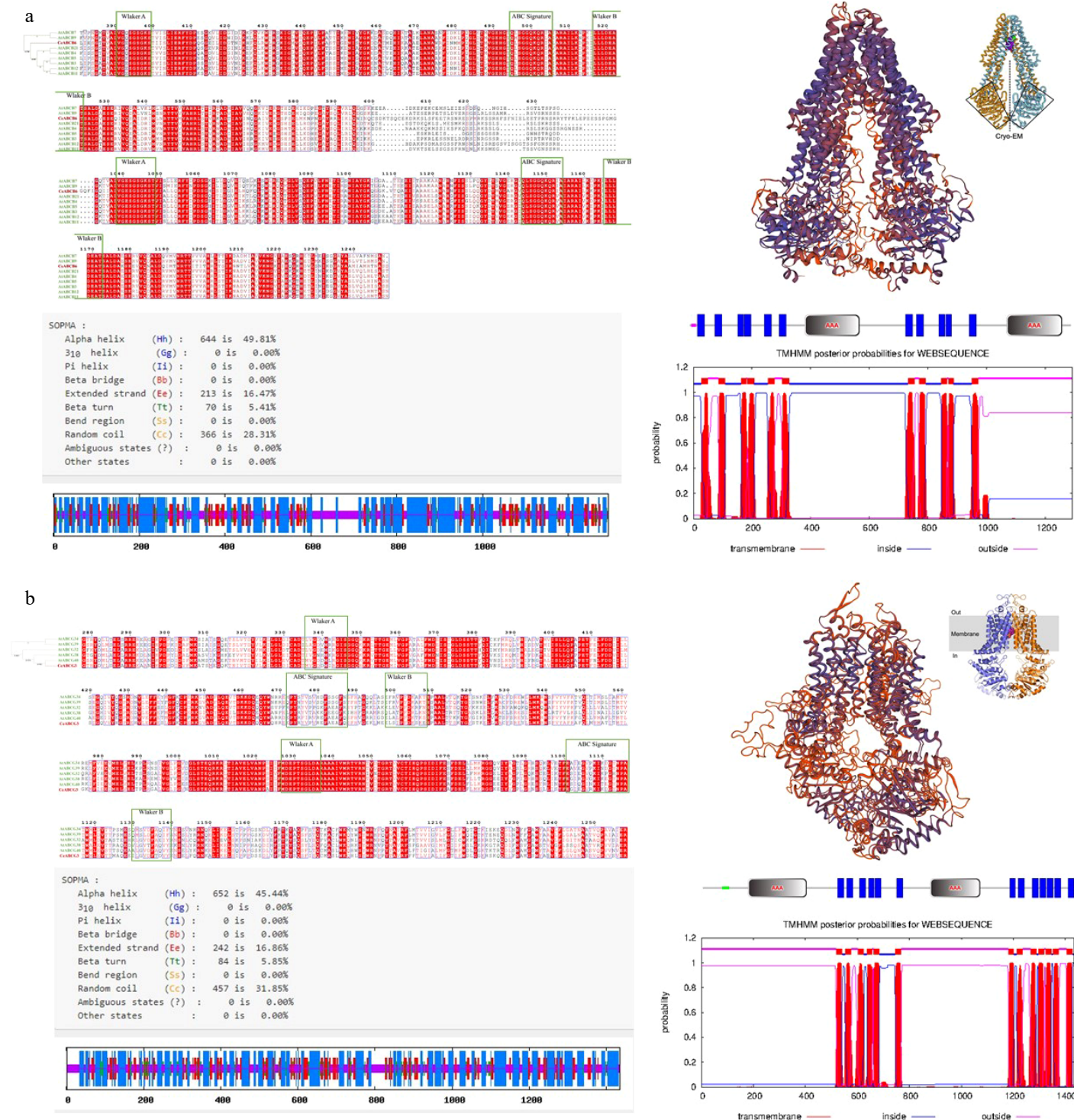


**Fig. 4** Structural prediction and subcellular localization of CeABCB6 and CeABCG3. (a), (b) Amino acid sequence alignment, domain organization, transmembrane topology (TMHMM), and tertiary structure modeling of CeABCB6 and CeABCG3, respectively.



(Supplementary Figs S3 & S4). Tertiary structure modeling further confirmed that both proteins possess the complete ABC transporter configuration, forming potential substrate-conducting pores across the membrane. These structural features strongly indicated *CeABCB6* and *CeABCG3* as full-length transporters involved in ATP-dependent metabolite translocation.

To validate their subcellular localization, GFP fusion constructs (*pCAMBIA1302-CeABCB6-GFP* and *pCAMBIA1302-CeABCG3-GFP*) were transiently expressed in *Nicotiana benthamiana* leaves. Confocal imaging revealed that GFP fluorescence from the control vector (*pCAMBIA1302-GFP*) was detected in both the plasma membrane and nucleus (Fig. 5a–c). In contrast, the fluorescence signals from the CeABC-GFP fusion proteins were exclusively associated with the plasma membrane (Fig. 5d–i), consistent with their predicted membrane transporter nature. Moreover, the fluorescence appeared stronger and more continuous than that of the control, suggesting effective membrane targeting and accumulation.

Taken together, these findings confirmed that *CeABCB6* and *CeABCG3* encode membrane-localized ABC transporters with structurally conserved features and strong potential for ATP-driven transmembrane transport of signaling molecules.

### Analysis of upstream and downstream regulation of *CeABC* gene expression over time

To further identify ABC transcription factors with MeJA transport capabilities from the initially screened candidates (*CeABCG3*, *CeABCG54*, *CeABCB6*, and *CeABCB30*), this study examined their diurnal expression patterns during the fourth and fifth days of *C. ensifolium* flowering (Fig. 6a). The results revealed that *CeABCB6* and *CeABCG3* exhibited peak expression levels at 8:00 a.m., with decreased expression at 12:00 and 16:00 as temperatures increased. Expression levels gradually recovered during the night, consistent

with previous findings on the diurnal scent emission rhythm in orchid species. In exogenous MeJA treatments of fully bloomed *C. ensifolium* flowers (blooming day 4), and during extended expression analyses (Fig. 6b, c), both genes showed varying degrees of up-regulation at 48 h (blooming day 6) compared to water-treated controls. However, by 96 h (blooming day 8), no significant differences were observed between experimental and control groups. This indicates that elevated MeJA concentrations may feedback-regulate the expression of these key *CeABC* genes, allowing them to respond actively to external MeJA fluctuations and fulfill biological functions. To verify the driving forces behind the expression of these *CeABCs*, the study simulated various abiotic stresses (Fig. 6d). Results showed that under auxin treatment, drought stress, and cold stress, *CeABCB6* expression was consistently down-regulated. Similarly, *CeABCG3* expression was down-regulated under drought stress, while auxin treatment led to increased expression over longer durations. Interestingly, during short-term cold stress, *CeABCG3* expression remained unchanged, but prolonged cold exposure significantly up-regulated its expression. This suggests that *C. ensifolium* may activate *CeABCG3* expression to promote MeJA release, potentially aiding in low-temperature stress responses.

Finally, the study analyzed correlations between the expression of these genes, endogenous and exogenous MeJA levels, and JA content during flower development to identify the *CeABC* transcription factors most involved in MeJA transmembrane transport. The results (Fig. 6e) showed a negative correlation between *CeABCB6* expression and MeJA release, while *CeABCG3* expression exhibited a positive correlation. The JA content showed minimal association with the expression of these two genes, whereas endogenous MeJA levels were positively correlated with JA content and *CeABCB6* expression but negatively correlated with *CeABCG3* expression.

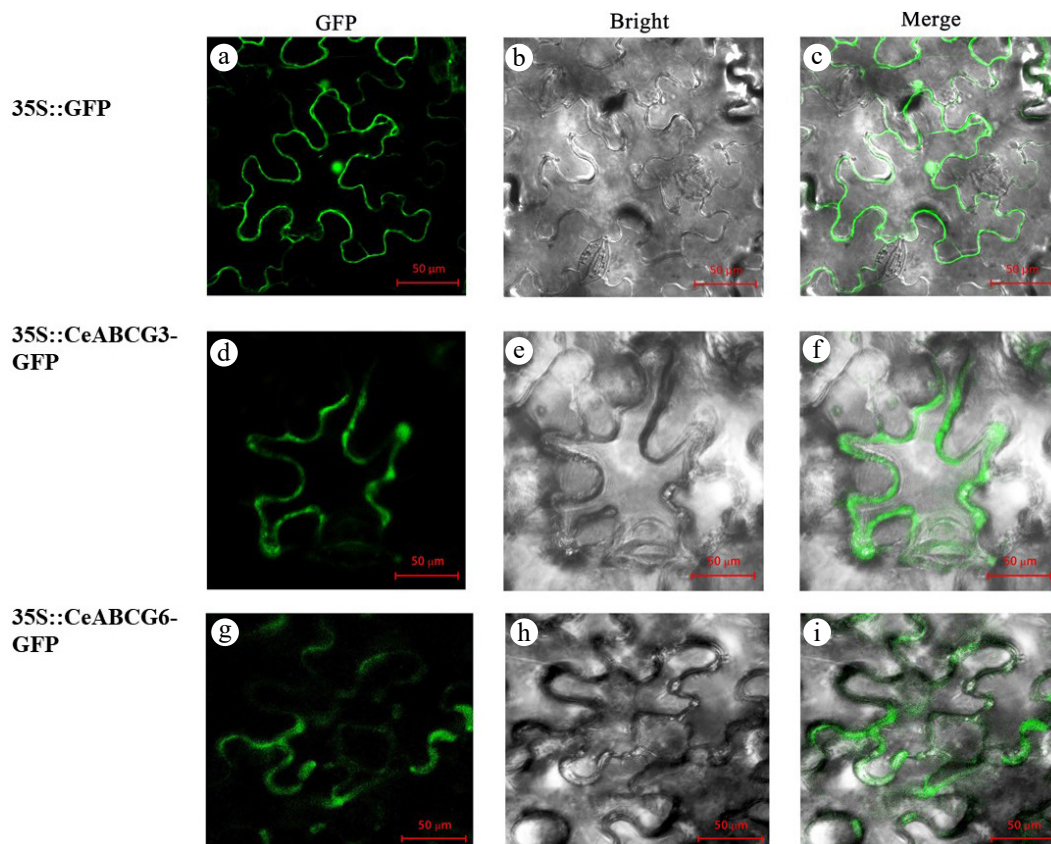


**Fig. 5** Subcellular localization of *CeABCB6*-GFP and *CeABCG3*-GFP fusion proteins in *Nicotiana benthamiana* leaves. (a)–(c) 1302-GFP control. (d)–(f) 1302-*CeABCG3*-GFP. (g)–(i) 1302-*CeABCB6*-GFP. GFP, bright field, and merged channels are shown.

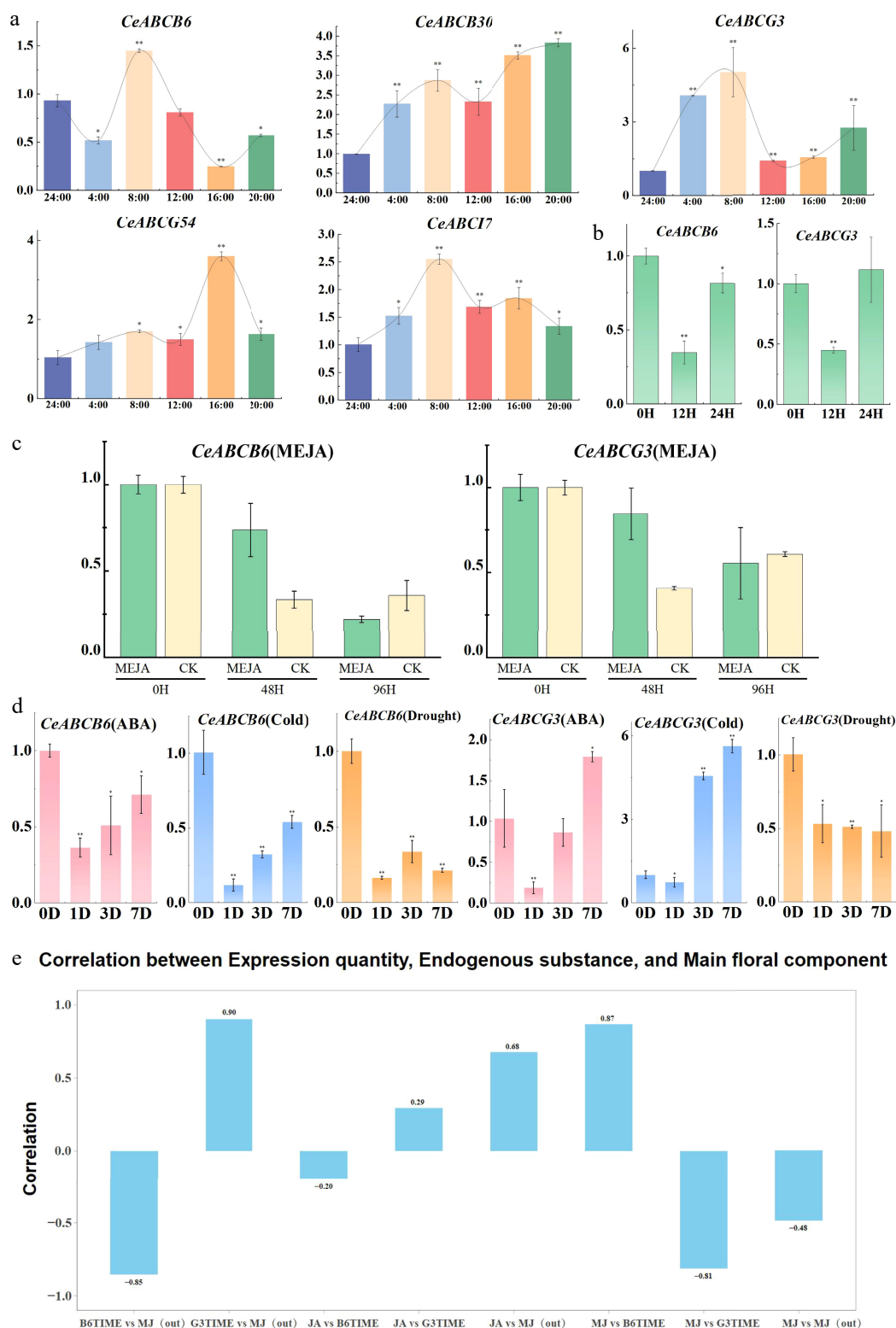


**Fig. 6** Expression changes of *CeABC* genes under various conditions and their correlation with MeJA release. (a) Diurnal expression patterns of *CeABC* genes during flower blooming. (b) Relative expression changes of *CeABC6* and *CeABCG3* under short-term MeJA treatment. (c) Relative expression changes of *CeABC6* and *CeABCG3* under prolonged MeJA treatment, with CK serving as the untreated control. (d) Expression changes of *CeABC6* and *CeABCG3* under various abiotic stresses. (e) Correlation analysis between *CeABC6* and *CeABCG3* expression levels and MeJA release during flower blooming.

## Discussion

### Components of floral fragrance and floral structure

Microscopic observation of the *C. ensifolium* tepals revealed that

the epidermal surface is smooth, lacking stomata and trichomes. The epidermal and secondary epidermal cells are rich in vacuoles, with large vacuoles compressing the organelles to the periphery of the cells, promoting the synthesis and release of volatile

compounds. During full bloom, plastids within these cells accumulate osmophilic granules, which are observable under electron microscopy. These granules may serve as precursors for aroma compounds and are highly correlated with the pattern of floral scent release<sup>[35]</sup>. Unlike species with specialized structures for volatile release, *C. ensifolium* may employ a membrane-mediated mechanism for the transport of volatiles, a process likely similar to the mechanism in *Petunia hybrid*, where floral scent compounds are transported across membranes via ABC transporters. Further ultra-structural analysis and functional studies of the CeABC transcription factors support this hypothesis, suggesting that non-structural cell components play a crucial role in volatile compound transport, which aligns with the physiological and molecular dynamics of floral scent release. In addition to changes in transporter gene expression, cold and drought stress have also been shown to directly influence floral scent emission. Stress conditions may alter membrane permeability, enzymatic activity, or precursor availability, thereby affecting the biosynthesis and release efficiency of volatile compounds. In particular, MeJA, as a volatile signal molecule, plays a dual role in stress signaling and scent emission. Under low-temperature or drought stress, the increased MeJA transport activity—partially mediated by CeABCG3 and CeABCB6—may lead to elevated endogenous MeJA levels in floral tissues, which could in turn modulate the expression of terpene synthase or other aroma-related genes. This complex interplay suggests that the floral scent emission of *C. ensifolium* is not only developmentally regulated, but also dynamically influenced by environmental cues, especially abiotic stresses such as cold and drought.

### Sequence analysis and transcriptional expression of CeABC genes related to floral scent

ABC transporters are an important family of membrane proteins that are widely involved in the transmembrane transport of plant secondary metabolites<sup>[36]</sup>. In *C. ensifolium*, these transporters retain conserved nucleotide-binding domains (NBDs) and subfamily-specific transmembrane domains (TMDs), reflecting their functional diversity. A whole-genome study has identified 121 ABC genes in *C. ensifolium*, with the ABCG and ABCB subfamilies being the most abundant<sup>[31]</sup>. G-type transporters play a key role in the transport of volatile substances, with previous studies showing that AtABCG1 and AtABCG16 in *Arabidopsis thaliana* mediate the transmembrane transport of jasmonic acid (JA) and its methyl ester (MeJA).

In *C. ensifolium* 'Xiaotaohong', transcriptomic analysis showed that CeABCB6 and CeABCG3 are predominantly expressed in the petals and sepals, which aligns with the specific release sites of the major floral scent compound (MeJA) in the variety. Furthermore, the diel rhythmic expression of these two genes is highly correlated with the dynamic release of floral scent, suggesting their key role in the transport of MeJA. CeABCB6 encodes 1,293 amino acids and contains two TMD-NBD structural domains, while CeABCG3 encodes 1,435 amino acids with an inverted NBD-TMD structure. It is speculated that these genes may mediate the transport of oppositely charged substrates. The spatiotemporal expression characteristics of these genes suggest that they might precisely regulate MeJA levels through an ATP-dependent transmembrane transport mechanism.

This study reveals the dual role of MeJA in *C. ensifolium* as both a floral scent volatile and a stress-response hormone. CeABCB6 and CeABCG3 play key roles in MeJA transport, collaboratively regulating floral scent production and environmental adaptation. The time lag observed between peak gene expression and the maximum release of volatiles suggests the presence of potential post-transcriptional regulation or intermediate steps in the transport process. This finding aligns with previous studies on the regulatory

mechanisms of ABC transporters. In the case of MeJA transport, the regulation of CeABCG3 and CeABCB6 may extend beyond the transcriptional level, with post-transcriptional regulation or intracellular membrane signal transduction possibly serving as crucial regulatory mechanisms in MeJA transport.

ABC transporters are widely known to mediate the transmembrane transport of hormones, metabolites, and resistance-related compounds in plants (AtABCB1, AtABCG1). Further research indicates that CeABCG3 and CeABCB6 facilitate MeJA transmembrane transport, with CeABCG3 playing a particularly prominent role in outward transport, a function consistent with other known ABC transporters. Similar studies on environmental adaptability have also been reported for other ABC transporters, such as the up-regulation of AtABCG1 under salt stress and the regulatory role of AtABCB4 under drought conditions. However, this study finds that CeABCG3 expression is significantly up-regulated under prolonged low-temperature stress, indicating that it may enhance MeJA transport capacity through mechanisms such as changes in membrane fluidity or activation of the ABA and Ca<sup>2+</sup> signaling pathways to cope with environmental changes.

### Conclusions

Solid-phase microextraction and CC-MS techniques identified 51, 59, and 67 volatile compounds from the flowers of *C. ensifolium* 'Xiaotaohong' at the early, full, and senescent flowering stages, respectively. Methyl jasmonate and  $\beta$ -caryophyllene, derived from fatty acids and terpenes, were the most abundant compounds in all stages. Microscopic observation of the fragrance-producing cells showed that during early blooming, large vacuoles occupied most of the epidermal cells in the sepals, with organelles positioned near the cell membrane. In full bloom, the organelles were more developed and concentrated near the membrane, with a large accumulation of lipophilic osmium particles in plastids. It was inferred that the epidermal and subepidermal cells of the sepals and petals were involved in fragrance production. CeABCB6 and CeABCG3, were highly expressed in the sepals and petals and exhibited a diurnal rhythm. These genes might be the key in the transport of fragrance compounds located in the cell membrane. Future experiments, including overexpression studies in MeJA-enriched plants and yeast functional assays, will further reveal their specific roles in the transport of volatile compounds.

### Author contributions

The authors confirm contributions to the paper as follows: conceptualization, methodology, supervision, writing, review and editing: Zhao K, Zhou Y; data curation, writing—original draft preparation: Peng Y, Zhan S, Cao Y; resources: Huang R, Zhao Y, Tang F, Wu H, Li X. All authors reviewed the results and approved the final version of the manuscript.

### Data availability

The raw genome data and assembled *C. ensifolium* genome were submitted to the National Genomics Data Center (NGDC) database with the accession number PRJCA005355/CRA004327 and GWHBCII00000000. The raw transcriptome sequences have been deposited in BioProject of GSA under the accession codes PRJCA009885/CRA007101 and PRJCA005426/CRA004351, respectively. All data generated or analyzed during this study are included in this published article and its supplementary information files, and also available from the corresponding author on reasonable request.



## Acknowledgments

The Project of National Key R&D Program (Grant No. 2023YFD1600504), Fujian Provincial Natural Science Foundation of China (Grant Nos 2023J01283, 2022J01639), the National Natural Science Foundation of China (Grant Nos 32101583, 31901353), the Innovation and Application Engineering Technology Research Center of Ornamental Plant Germplasm Resources in Fujian Province (Grant No. 115-PJH16005), the Key Research and Development Program of the Ningxia Hui Autonomous Region in China (Grant No. 2022BBF02041). We would like to thank the editor and reviewers for their helpful comments on the manuscript.

## Conflict of interest

The authors declare that they have no conflict of interest.

**Supplementary information** accompanies this paper at (<https://www.maxapress.com/article/doi/10.48130/opr-0025-0031>)

## Dates

Received 30 December 2024; Revised 24 June 2025; Accepted 3 July 2025; Published online 2 September 2025

## References

- Hao R, Yang S, Zhang Z, Zhang Y, Chang , et al. 2021. Identification and specific expression patterns in flower organs of ABCG genes related to floral scent from *Prunus mume*. *Scientia Horticulturae* 288:110218
- Maiti S, Mitra A. 2017. Morphological, physiological and ultrastructural changes in flowers explain the spatio-temporal emission of scent volatiles in *Polianthes tuberosa* L. *Plant and Cell Physiology* 58:2095–111
- Liu Y, Jing SX, Luo SH, Li SH. 2019. Non-volatile natural products in plant glandular trichomes: chemistry, biological activities and biosynthesis. *Natural Product Reports* 36:626–65
- Yin H, Yin J, Liao Y, Lu S, Li C. 2021. Phenotype classification based on flower color, pigment distribution and epidermal cell shape of dendrobium hybrids. *Acta Horticulturae Sinica* 48:1907–20
- Dang X, Chen B, Liu F, Ren H, Liu X, et al. 2020. Auxin signaling-mediated apoplastic pH modification functions in petal conical cell shaping. *Cell Reports* 30:3904–3916.e3
- Adebesin F, Widhalm JR, Boachon B, Lefèvre F, Pierman B, et al. 2017. Emission of volatile organic compounds from petunia flowers is facilitated by an ABC transporter. *Science* 356:1386–88
- Skaliter O, Kitsberg Y, Sharon E, Shklarman E, Shor E, et al. 2021. Spatial patterning of scent in petunia corolla is discriminated by bees and involves the ABCG1 transporter. *The Plant Journal* 106:1746–58
- Do THT, Martinoia E, Lee Y. 2018. Functions of ABC transporters in plant growth and development. *Current Opinion in Plant Biology* 41:32–38
- Zhou Y, Wang Y, Zhang D, Liang J. 2024. Endomembrane-biased dimerization of ABCG16 and ABCG25 transporters determines their substrate selectivity in ABA-regulated plant growth and stress responses. *Molecular Plant* 17:478–95
- Charton L, Plett A, Linka N. 2019. Plant peroxisomal solute transporter proteins. *Journal of Integrative Plant Biology* 61:817–35
- Li M, Yu G, Cao C, Liu P. 2021. Metabolism, signaling, and transport of jasmonates. *Plant Communications* 2:100231
- Li Q, Zheng J, Li S, Huang G, Skilling SJ, et al. 2017. Transporter-mediated nuclear entry of jasmonoyl-isoleucine is essential for jasmonate signaling. *Molecular Plant* 10:695–708
- Eberl F, Gershenzon J. 2017. Releasing plant volatiles, as simple as ABC. *Science* 356:1334–35
- Garcia O, Bouige P, Forestier C, Dassa E. 2004. Inventory and comparative analysis of rice and *Arabidopsis* ATP-binding cassette (ABC) systems. *Journal of Molecular Biology* 343:249–65
- Yu J, Ge J, Heuveling J, Schneider E, Yang M. 2015. Structural basis for substrate specificity of an amino acid ABC transporter. *Proceedings of the National Academy of Sciences of the United States of America* 112:5243–48
- Fu S, Lu YS, Zhang X, Yang GZ, Chao D, et al. 2019. The ABC transporter ABCG36 is required for cadmium tolerance in rice. *Journal of Experimental Botany* 70:5909–18
- Lopez-Ortiz C, Dutta SK, Natarajan P, Peña-García Y, Abburi V, et al. 2019. Genome-wide identification and gene expression pattern of ABC transporter gene family in *Capsicum* spp. *PLoS One* 14:e0215901
- Ofori PA, Mizuno A, Suzuki M, Martinoia E, Reuscher S, et al. 2018. Genome-wide analysis of ATP binding cassette (ABC) transporters in tomato. *PLoS One* 13:e0200854
- Zhang XD, Zhao KX, Yang ZM. 2018. Identification of genomic ATP binding cassette (ABC) transporter genes and Cd-responsive ABCs in *Brassica napus*. *Gene* 664:139–51
- Huang J, Li X, Chen X, Guo Y, Liang W, et al. 2021. Genome-wide identification of soybean ABC transporters relate to aluminum toxicity. *International Journal of Molecular Sciences* 22:6556
- Hwang JU, Song WY, Hong D, Ko D, Yamaoka Y, et al. 2016. Plant ABC transporters enable many unique aspects of a terrestrial plant's lifestyle. *Molecular Plant* 9:338–55
- Ying W, Wang Y, Wei H, Luo Y, Ma Q, et al. 2024. Structure and function of the *Arabidopsis* ABC transporter ABCB19 in brassinosteroid export. *Science* 383:eadj4591
- Gräfe K, Schmitt L. 2021. The ABC transporter G subfamily in *Arabidopsis thaliana*. *Journal of Experimental Botany* 72:92–106
- Kuromori T, Sugimoto E, Shinozaki K. 2011. *Arabidopsis* mutants of AtABCG22, an ABC transporter gene, increase water transpiration and drought susceptibility. *The Plant Journal* 67:885–94
- Kang J, Yim S, Choi H, Kim A, Lee KP, et al. 2015. Absciscic acid transporters cooperate to control seed germination. *Nature Communications* 6:8113
- Ko D, Kang J, Kiba T, Park J, Kojima M, et al. 2014. *Arabidopsis* ABCG14 is essential for the root-to-shoot translocation of cytokinin. *Proceedings of the National Academy of Sciences of the United States of America* 111:7150–55
- An N, Huang X, Yang Z, Zhang M, Ma M, et al. 2024. Cryo-EM structure and molecular mechanism of the jasmonic acid transporter ABCG16. *Nature Plants* 10:2052–61
- Aragón W, Reina-Pinto JJ, Serrano M. 2017. The intimate talk between plants and microorganisms at the leaf surface. *Journal of Experimental Botany* 68:5339–50
- Ziv C, Zhao Z, Gao YG, Xia Y. 2018. Multifunctional roles of plant cuticle during plant-pathogen interactions. *Frontiers in Plant Science* 9:1088
- Chen J, Zhu X, Zheng R, Tong Y, Peng Y, et al. 2024. Orchestrating of native *Phalaenopsis* flower scents lighted the way through artificial selective breeding partiality in the current resource utilization. *Industrial Crops and Products* 217:118850
- Cao YH, Hu MJ, Tong Y, Zhang YP, Zhao K, et al. 2022. Identification of the ABC gene family and expression pattern analysis during flower development in *Cymbidium ensifolium*. *Biotechnology Bulletin* 38:162–74
- Feng Z, Li M, Li Y, Wan X, Yang X. 2020. Characterization of the orchid-like aroma contributors in selected premium tea leaves. *Food Research International* 129:108841
- Hong Y, Ahmad N, Zhang J, Lv Y, Yao N. 2023. The CtMYB63-CtU-box1-CtUCH1 module regulates cold tolerance and Hydroxysafflower yellow A accumulation in *Carthamus tinctorius*. *Industrial Crops and Products* 202:117088
- Zhang Q, Ahmad N, Li Z, He J, Wang N, et al. 2023. CtCYP71A1 promotes drought stress tolerance and lignin accumulation in safflower and *Arabidopsis*. *Environmental and Experimental Botany* 213:105430
- Zhou L, Wu S, Chen Y, Huang R, Cheng B, et al. 2024. Multi-omics analyzes of *Rosa gigantea* illuminate tea scent biosynthesis and release mechanisms. *Nature Communications* 15:8469
- Banasiak J, Jasiński M. 2022. ATP-binding cassette transporters in non-model plants. *New Phytologist* 233:1597–612



Copyright: © 2025 by the author(s). Published by Maximum Academic Press, Fayetteville, GA. This article is an open access article distributed under Creative Commons Attribution License (CC BY 4.0), visit <https://creativecommons.org/licenses/by/4.0/>.